ACS APPLIED MATERIALS & INTERFACES

Research Article

www.acsami.org

Transformation of Polymer Nanofibers to Nanospheres Driven by the Rayleigh Instability

Yu-Chieh Huang, Ping-Wen Fan, Chih-Wei Lee, Chien-Wei Chu, Chia-Chan Tsai, and Jiun-Tai Chen*

Department of Applied Chemistry, National Chiao Tung University, Hsinchu, Taiwan 30050

Supporting Information

ABSTRACT: We study the thermal annealing effect of poly(methyl methacrylate) (PMMA) nanofibers made from anodic aluminum oxide (AAO) templates and their transformation to PMMA nanospheres. The PMMA nanofibers are prepared by wetting an AAO template with a 30 wt % PMMA solution, followed by the evaporation of the solvent. After the AAO template is removed by a weak base, the PMMA nanofibers are thermally annealed in ethylene glycol, a nonsolvent for PMMA. The surfaces of the nanofibers undulate and transform into nanospheres, driven by the Rayleigh instability. The driving force for the transformation process is the minimization of the interfacial energy between PMMA nanofibers and ethylene glycol. The transformation times at higher annealing temperatures are shorter than those at lower annealing temperatures. This study provides a facile route to prepare polymer nanospheres which are not accessible by other traditional methods.

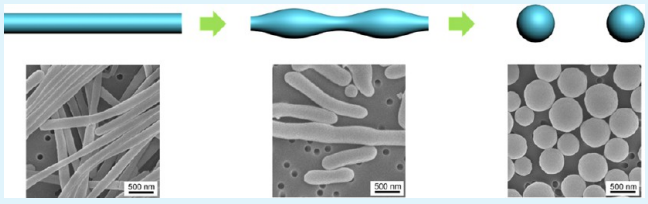

KEYWORDS: *annealing, nanofibers, nanospheres, PMMA, templates*

INTRODUCTION

Polymer nanomaterials have attracted much attention in recent years because of their applications in areas such as actuators, sensors, drug delivery, or organic solar cells.[1−4] These applications are related to the unique properties and morphologies of different types of polymer nanomaterials. Various methods have been developed to fabricate polymer nanomaterials such as electrospinning, electron beam lithography, dip-pen nanolithography, and the template method.[5−8] Compared with other methods, the template method has been shown to be a versatile technique to prepare various kinds of polymer nanomaterials.[9−14] In a typical template method, polymer solutions or melts are introduced into the nanopores of a porous template, and polymer nanomaterials are obtained after the template is selectively removed. A key feature of the template method is that the sizes of the nanomaterials are controlled by the sizes of the nanopores of the templates. By using templates, polymer nanomaterials with unique properties and unusual morphologies, which are not accessible in the bulk state, have been obtained.[15]

Porous anodic aluminum oxide (AAO) is widely used as templates for fabricating various kinds of nanomaterials. The AAO templates are prepared by the electrochemical oxidation of aluminum, and hexagonally packed nanopores with high pore densities can be obtained by using a two-step anodization process.[16] The pore diameters, pore-to-pore distances, and thicknesses of the AAO templates are controlled by the anodization conditions such as the electrolyte solution type, the electrolyte concentration, the working temperature, the anodization voltage, or the anodization time.[17,18]

Although many polymer nanomaterials have been prepared by using templates such as the AAO templates, the annealing effect on the morphology changes of the polymer nanomaterials has been little studied. For example, Russell et al. recently studied the dewetting behavior of polystyrene (PS) films confined within the cylindrical nanopores of an AAO template by annealing the sample above the glass transition temperature.[19] Polymer nanostructures (nanorods and nanospheres) can be prepared and controlled by changing the initial film thickness and the surface properties of the cylindrical nanopores. Here, we study the preparation of poly(methyl methacrylate) (PMMA) nanofibers using AAO templates and investigate the transformation process of polymer nanofibers to nanospheres upon thermal annealing. PMMA nanofibers are prepared by wetting an AAO template with a PMMA solution. Water is added to the polymer solution confined in the nanopores of the AAO templates, resulting in the formation of polymer nanofibers.[20] After being released from the AAO template, the PMMA nanofibers are thermally annealed in ethylene glycol, a nonsolvent for PMMA. Upon thermal annealing, the surfaces of the nanofibers undulate, and the nanofibers transform to polymer nanospheres, driven by the Rayleigh instability.[21]

The Rayleigh instability is a phenomenon commonly seen in our daily life. For instance, when a column of water is falling from a kitchen faucet, it breaks up into tiny droplets. Plateau pioneered the study of instabilities in liquid cylinders.[22] He

Received: January 4, 2013
Accepted: March 20, 2013
Published: March 20, 2013

realized that the instability of a liquid cylinder is a result of the liquid surface tension. For a liquid cylinder with a radius of R_0, its surface undulates with a wavelength λ, and the total surface area decreases when λ is larger than the perimeter of the liquid cylinder ($2\pi R_0$). The surface undulation amplifies, resulting in the formation of a chain of liquid drops. Following the instability work, Rayleigh showed that the wavelength of the surface undulation is controlled by the fastest undulation mode.[23] Tomotika later extended this theory to the breakup of Newtonian liquid cylinders in a Newtonian liquid matrix.[24] He found that the time required for the cylinder breakup is related to parameters such as the interfacial tension, the viscosity ratio, and the initial radius of the cylinder. The Rayleigh-instability-type transformation was applied to solid cylinders by Nichols and Mullins, who studied the mass transport of solid cylinders.[25] They calculated the wavelengths of maximum growth rates by considering either surface or volume diffusion. For a cylinder with a radius of R_0, an infinitesimal longitudinal sinusoidal perturbation is introduced. The equation of the perturbed surface is given by

$$r = R_0 + \delta \sin(2\pi/\lambda)z \quad (1)$$

where δ is the amplitude of the perturbation, λ is the wavelength of the perturbation, and the z axis coincides with the cylindrical axis. As long as the wavelength of the perturbation $\lambda > 2\pi R_0$, the amplitude increases spontaneously with time. For surface diffusion, which dominates in most cases, the perturbation with the maximum growth rate has a wavelength $\lambda_m = 2\pi\sqrt{2}R_0 = 8.89R_0$.[25] The amplitude of the perturbation with the maximum growth rate continues to increase, and the cylinder eventually breaks up into a line of spheres with a spacing $\sim \lambda_m$.

The Rayleigh-instability-type transformation is observed for metal nanomaterials. Toimil Molares et al. studied the fragmentation of copper nanowires driven by the Rayleigh instability.[26] The copper nanowires are annealed at 600 °C on a SiO_2 substrate and decay into a chain of nanospheres with a spacing which is in agreement with the theoretical calculation. The Rayleigh-instability-type transformation is also observed for polymer nanomaterials.[27−31] For example, Park et al. reported the fabrication of highly ordered Teflon nanospheres driven by the Rayleigh instability.[28] A sawtoothed PDMS pattern is first placed on a spin-coated Teflon film, followed by an annealing process. Different sizes and separation distances of the nanospheres can be obtained by changing the pitches and amplitudes of the sawtoothed patterns.[28] He et al. studied the assembled polyelectrolyte nanotubes composed of poly(styrenesulfonate) and poly(allylamine hydrochloride) multilayers by the layer-by-layer deposition.[27] After high-temperature treatment in an aqueous phase, the polyelectrolyte multilayers transform from nanotubes to capsules. The shrinkage of the transformed capsules is also observed and accompanied by a decrease of the surface area of the capsules and an increase of the wall thickness.[27] Russell et al. also studied the Rayleigh-instability-driven transformation process of thin polymer films confined within a nanoporous alumina membrane upon thermal annealing.[29,30] After thermal annealing, the polymer films undulate and bridge across the cylindrical nanopores, resulting in the formation of polymer nanorods with periodic encapsulated holes.[29] For most of these studies, the polymer nanomaterials are placed on substrates during the transformation process. Therefore, the Rayleigh-instability-driven transformation process is perturbed by the underlying substrate.

Here, we study the annealing effect of PMMA nanofibers made by AAO templates. The substrate effect is prevented by annealing the PMMA nanofibers in ethylene glycol. Ethylene glycol provides an environment for annealing the nanofibers uniformly.[32] Upon thermal annealing, PMMA nanofibers undulate and transform to PMMA nanospheres. The morphology change depends on the annealing temperature and the annealing time.[32,33] The transformation time at higher annealing temperature is shorter than the time at lower annealing temperature because of the lower viscosity. Considering the versatility of template-based nanomaterials, this transforming concept can be applied to other materials or structures such as block copolymers, polymer blends, metals, or inorganic materials.

EXPERIMENTAL SECTION

Materials. Poly(methyl methacrylate) (PMMA) (M_w: 97 kg mol^{-1}) was purchased from Sigma-Aldrich. *N*,*N*-dimethylformamide (DMF) was obtained from Tedia. Sodium hydroxide (NaOH) was obtained from Showa. Ethylene glycol was purchased from Scharlab. Wipers (Kimwipes) were obtained from Kimberly-Clark. Polycarbonate filters (VCTP, pore size: 0.1 μm) were purchased from Millipore. Anodic aluminum oxide (AAO) templates (pore diameter ~ 150−400 nm, thickness ~ 60 μm) were purchased from Whatman. The AAO templates were cleaned by acetone and dried before use.

Fabrication of PMMA Nanofibers from AAO Templates. The AAO templates were first immersed into PMMA solutions (PMMA in DMF, 30 wt %) for 10 s. After the templates were taken out of the polymer solution, the residual solution outside the nanopores of the AAO templates was removed by wiping with wipers (Kimwipes). Subsequently, the AAO templates were then dipped into a bottle of deionized water for 10 min.[20] The AAO templates were then selectively dissolved by NaOH(aq). Finally, the samples were filtered and washed with deionized water using polycarbonate filters.

Annealing Process of PMMA Nanofibers. After the PMMA nanofibers were collected, they were placed in a 10 mL round-bottom flask containing 3 mL of ethylene glycol, which was preheated to a desired temperature. During the annealing process, a magnetic stir bar was used to stir the solution at a constant speed of 200 rpm. After the nanofibers were annealed for the desired periods of time, they were cooled down and washed by deionized water, followed by filtration using polycarbonate filters.

Structure Analysis and Characterization. The glass temperatures (T_g) of the polymers were investigated by differential scanning calorimetry (DSC) using a SEIKO Instruments EXSTAR 6000 DSC. The samples before and after thermal annealing were characterized by a JEOL JSM-7401F scanning electron microscope (SEM) at an accelerating voltage of 5 kV. The samples were coated with 4 nm platinum before the SEM measurement. Bright-field transmission electron microscopy (TEM) studies were also conducted with a JEOL JEM-2010 TEM operating at an accelerating voltage of 200 kV. For TEM measurement, the samples were placed onto copper grids coated with carbon films.

RESULTS AND DISCUSSION

Figure 1 shows the schematic illustration of the fabrication process of PMMA nanofibers and their transformation to nanospheres. The PMMA nanofibers are first prepared by wetting an AAO template with a 30 wt % PMMA solution. The SEM images and the pore size distribution of the AAO templates are shown in the Supporting Information. The average pore size of the AAO template is 237 nm. The PMMA solution wets the nanopores of the AAO template by capillary force. For a liquid wetting a cylindrical pore, the height of the liquid cylinder is given by the Jurin's law

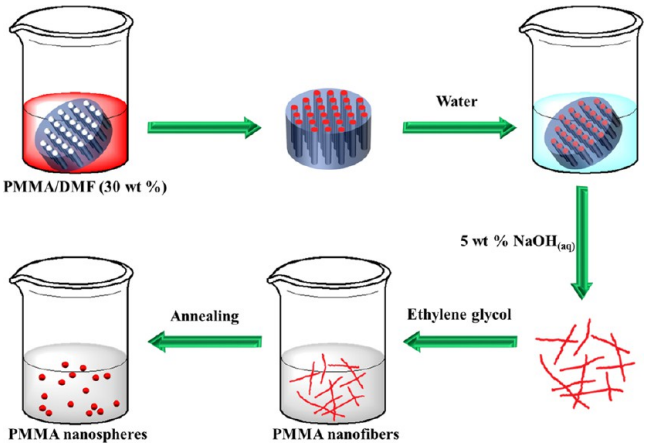

Figure 1. Schematic illustration of the fabrication process of PMMA nanofibers and nanospheres. The PMMA nanofibers are first made by AAO templates. After the nanofibers are annealed in ethylene glycol, they transform to nanospheres.

$$h = 2\gamma \cos\theta/\rho g r \quad (2)$$

where h is the height, γ is the surface tension of the liquid, θ is the contact angle, ρ is the density of the liquid, g is the gravity, and r is the radius of the pore.[34] Therefore, the height at which the polymer solution can reach in the pore is inversely proportional to the radius of the pore. The polymer solution is able to fill the nanopores of the AAO templates within seconds because of the small pore diameters (~150−400 nm) and the presence of the solvent.

After the AAO templates are taken out from the PMMA solution, a wiping step is performed to remove the residual solution outside the nanopores of the AAO templates. Without this step, thin layers of polymer films are formed outside the nanopores, and the annealing results are perturbed. The solution-containing AAO templates are then dipped into a bottle of deionized water to induce the formation of polymer nanofibers. Usually polymer nanotubes are formed by wetting a porous template with a polymer solution because of the precipitation of polymers on the pore walls. Recently, we have studied that a nonsolvent such as water can form a wetting layer on the surface of the pore wall of an AAO template, causing the polymer solution to be isolated in the center of the pores.[20] Consequently, polymer nanospheres or nanofibers can be obtained, depending on the polymer concentration. By adding water into 30 wt % PMMA solution confined in the nanopores of the AAO templates, PMMA nanofibers are obtained.

After the formation of the PMMA nanofibers, the AAO template is selectively removed by NaOH(aq). Previously, thermal annealing has been performed for polymer nanotubes confined within AAO templates, and the nanotubes transform into nanorods with periodic encapsulated holes.[29,30] But the transformation process is affected by the alumina surface. To study the transformation process of nanofibers by thermal annealing while avoiding the substrate effect, the PMMA nanofibers are thermally annealed in a flask containing ethylene glycol which is preheated to the desired annealing temperature. Ethylene glycol has a high boiling point (T_b = 197.3 °C) and provides an environment for annealing the nanofibers uniformly. The aggregation of the nanofibers during the annealing process is prevented by stirring the mixture. Without

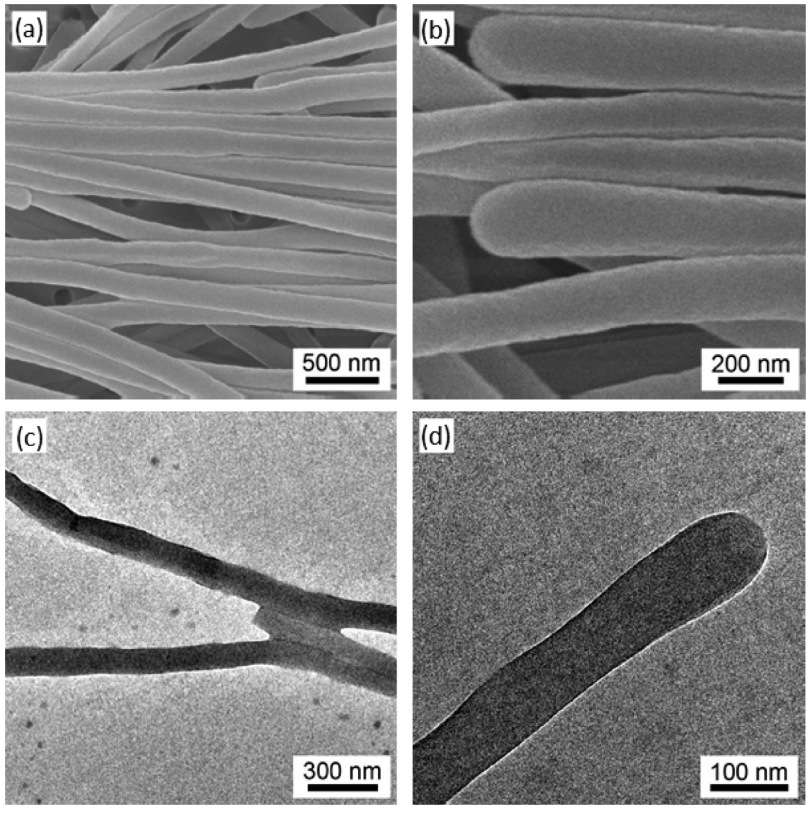

Figure 2. SEM and TEM images of PMMA (M_w: 97 kg mol^{-1}) nanofibers by using 30 wt % PMMA solution. (a, b) SEM images of PMMA nanofibers at different magnifications. (c, d) TEM images of PMMA nanofibers at different magnifications.

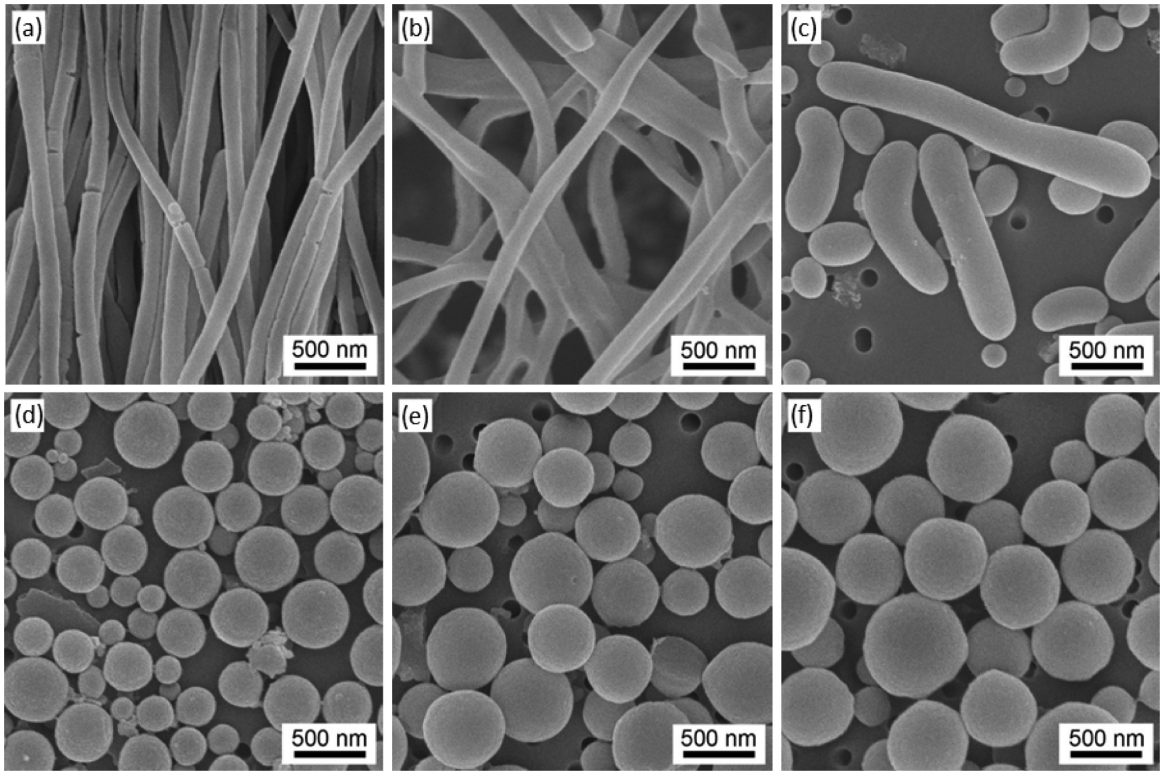

Figure 3. SEM images of PMMA nanostructures by annealing PMMA nanofibers in ethylene glycol for 3 h at different temperatures: (a) room temperature, (b) 80, (c) 90, (d) 100, (e) 120, and (e) 140 °C.

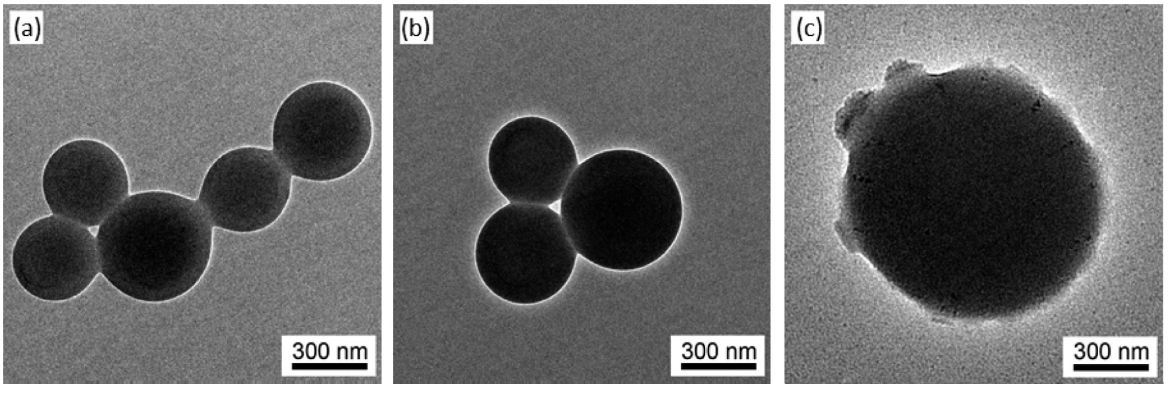

Figure 4. TEM images of PMMA nanospheres by annealing PMMA nanofibers in ethylene glycol at 120 °C for 1 h.

stirring, PMMA nanofibers aggregate and form bulk PMMA films after the annealing process. The transformation process is found to be independent of the stirring speed once the stirring speed is higher than a critical value. The stirring speed is fixed at 200 rpm for all the annealing experiments. After the nanofibers are annealed in ethylene glycol at the desired temperature for the desired time, the samples are cooled down while continuing the stirring. If the stirring is stopped before the samples are cooled down, the transformed nanospheres adhere to other nanospheres. Finally, the samples are washed with deionized water and filtered with polycarbonate filters, following by a drying process using a vacuum pump.

Parts a and b of Figure 2 are the SEM images of PMMA nanofibers made from the AAO templates. The hemispherical ends of the PMMA nanofibers are observed. The average diameters of the PMMA nanofibers are ~155 nm, smaller than the average pore diameter of the AAO template (~237 nm, see the Supporting Information). The reduction in size is because of the water-induced-aggregation of the polymer chains in the center of the nanopores.[20] Without adding water, the polymer chains precipitate on the pore walls, and polymer nanotubes are formed with the outer diameters close to the pore diameters of the templates. The internal structures of the PMMA nanofibers are examined by TEM, and the TEM images of PMMA nanofibers at different magnifications are shown in Figure 2c,d. The aspect ratio (the length divided by the diameter) of the polymer nanofibers has also been found to increase with the polymer concentration.[20]

To study the annealing effect on the PMMA nanofibers and their transformation to PMMA nanospheres, the PMMA nanofibers are released from the AAO templates and annealed in ethylene glycol for different periods of time at different temperatures. Figure 3 shows the SEM images of PMMA nanofibers annealed in ethylene glycol at different temperatures

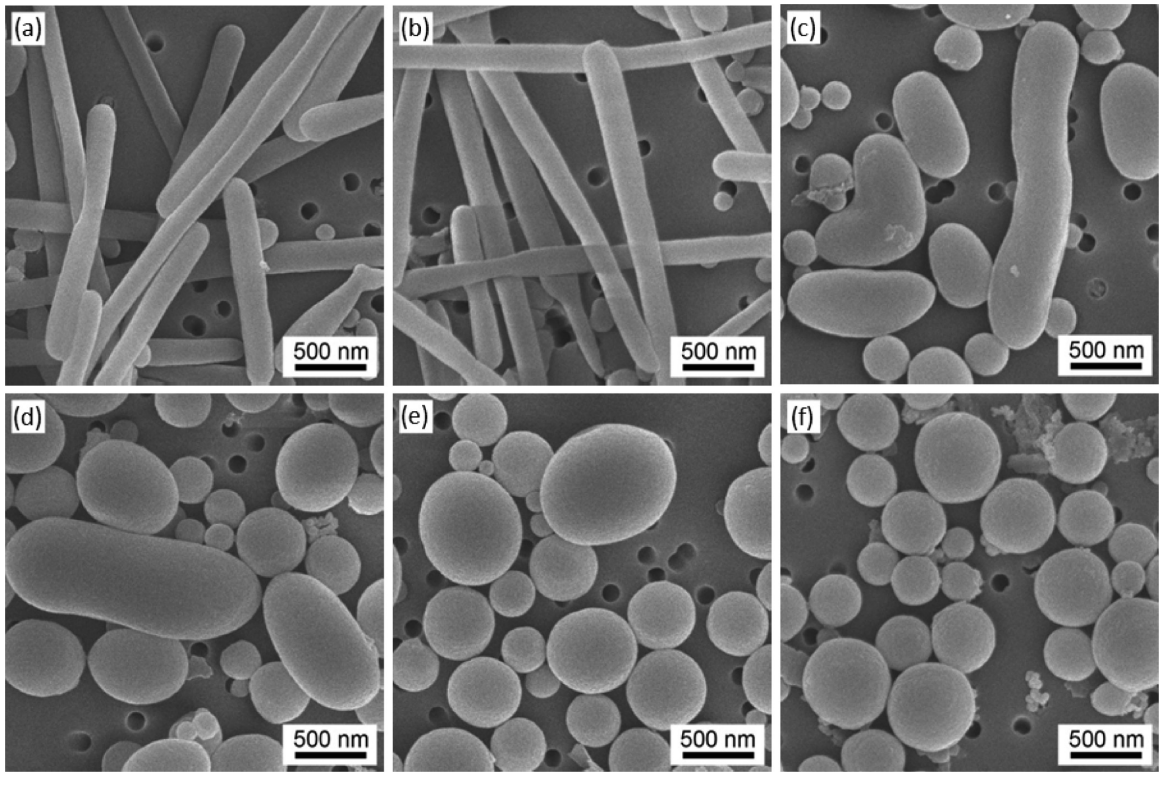

Figure 5. SEM images of PMMA nanostructures by annealing PMMA nanofibers in ethylene glycol at 100 °C for different periods of time: (a) 5, (b) 7, (c) 30, (d) 35, (e) 40, and (f) 45 min.

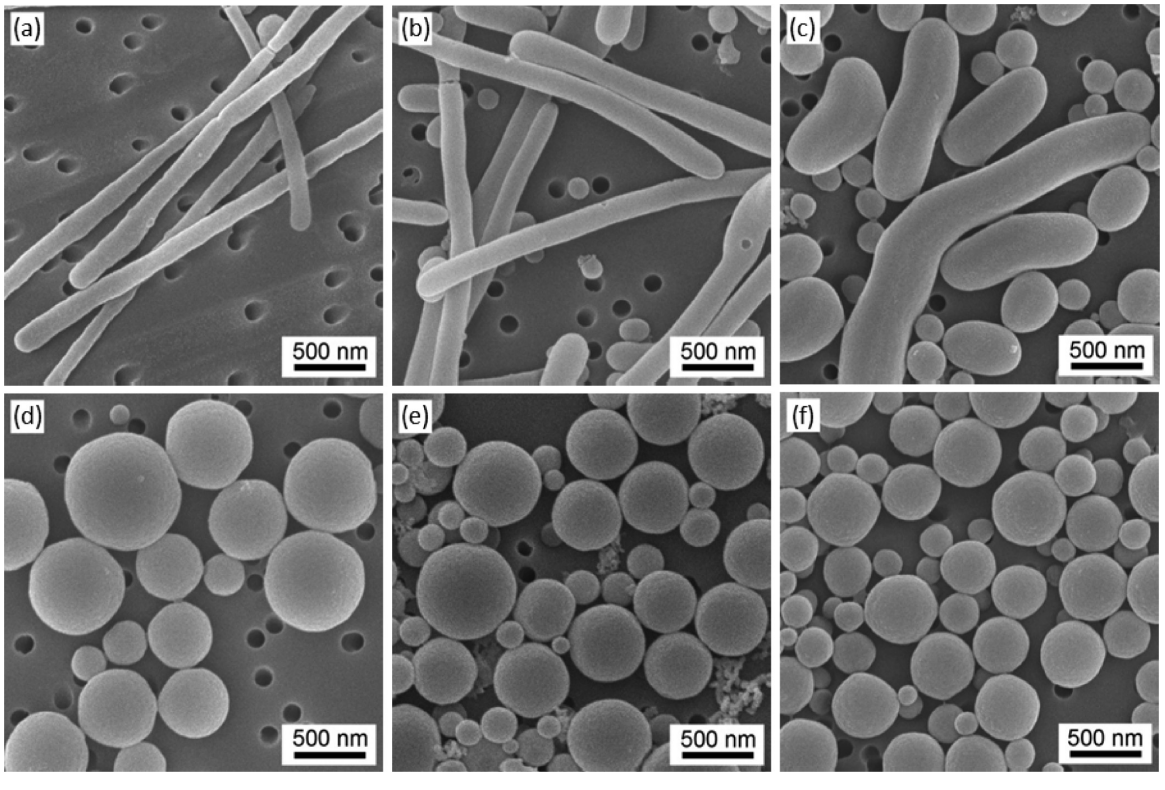

Figure 6. SEM images of PMMA nanostructures by annealing PMMA nanofibers in ethylene glycol at 120 °C for different periods of time: (a) 1, (b) 3, (c) 5, (d) 9, (e) 11, and (f) 30 min.

for 3 h. The fiber structures are retained when the samples are annealed at room temperatures for 3 h, as shown in Figure 3a. The bulk glass transition temperature (T_g) of PMMA used in this study is 108 °C, as determined by DSC. When the PMMA nanofibers are annealed at temperatures higher than the bulk T_g of the polymers, transformation from nanofibers to nano-

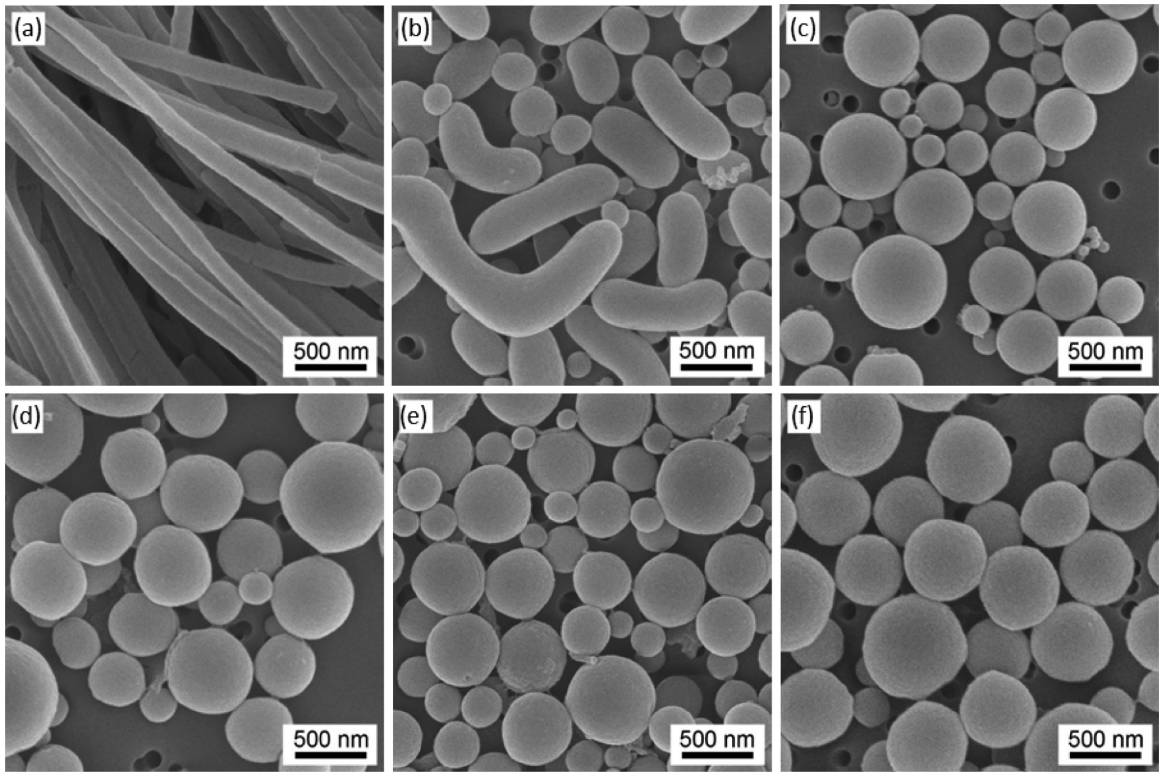

Figure 7. SEM images of PMMA nanostructures by annealing PMMA nanofibers in ethylene glycol at 140 °C for different periods of time: (a) 1 min, (b) 3 min, (c) 5 min, (d) 30 min, (e) 1 h, and (f) 3 h.

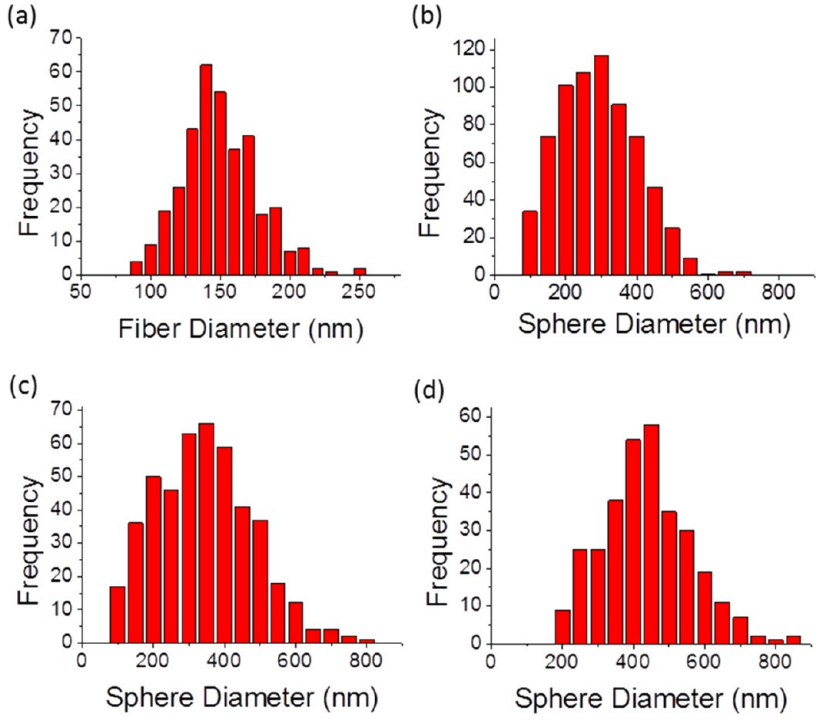

Figure 8. Size distribution histograms of PMMA nanostructures. (a) PMMA nanofibers made from AAO templates. (b–d) PMMA nanospheres by annealing PMMA nanofibers at 100 (b), 120 (c), and 140 °C (d).

spheres is observed. It has to be noted that the polymer chains near the fiber surface may have different T_g values from the bulk T_g because of the interface and chain confinement effects.[35,36] Therefore, the polymer chains near the center of the fibers may behave differently from those near the fiber surfaces.

Figure 3b–f shows the PMMA nanostructures annealed for 3 h at 80, 90, 100, 120, and 140 °C, respectively. The fiber morphology is still observed at lower annealing temperatures (room temperature to 80 °C). When the annealing temperature is increased to 90 °C, polymer nanorods or worm-like

dx.doi.org/10.1021/am400029j | ACS Appl. Mater. Interfaces 2013, 5, 3134–3142

(a)

Samples	A	B	C	D	E	F	G
Annealing Temperature (°C)	Without Annealing	100	110	120	130	140	150
Morphology	Fiber	Sphere	Sphere	Sphere	Sphere	Sphere	Sphere
Average size (nm)	155	317	411	367	452	463	397
Standard Deviation (nm)	27	110	136	135	150	127	110

(b)

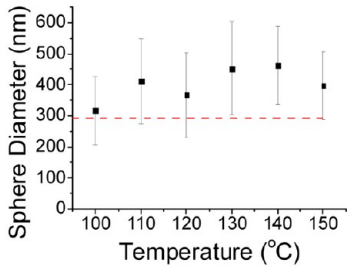

Figure 9. (a) Summary table of PMMA nanofibers annealed in ethylene glycol at different temperatures. (b) A plot of the nanosphere size versus the annealed temperature. The error bars represent standard deviations. The red dashed line indicates the calculated value of the nanospheres at 293 nm.

nanostructures are obtained. When the annealing temperatures are higher than 100 °C, most nanofibers transform to nanospheres. The solid nature of the nanospheres is further confirmed by TEM. Figure 4 shows the TEM images of PMMA nanospheres that are annealed at 120 °C for 1 h.

To investigate the details of the transforming process from nanofibers to nanospheres, the nanofibers are annealed at the same temperatures for different periods of time. Figure 5 shows the SEM images of PMMA nanostructures by annealing PMMA nanofibers in ethylene glycol at 100 °C for different periods of time. At shorter annealing times (0−15 min), the fiber morphology is retained. As the annealing time increases, worm-like nanostructures are observed, which can be identified as the intermediate structures during the transformation process, as shown in Figure 5c−e. At longer annealing times (>40 min), the nanofibers transform to nanospheres, as shown in Figure 5f. For higher annealing temperatures, similar time-dependent transformation processes are also observed. Figures 6 and 7 show the SEM images of PMMA nanostructures by annealing PMMA nanofibers in ethylene glycol at 120 and 140 °C, respectively. At higher annealing temperatures, the transformation process is found to occur at shorter times. The results of PMMA nanostructures by annealing PMMA nanofibers at other temperatures are shown in the Supporting Information, and similar transformation processes are observed.

If the fluid viscosity is neglected, the characteristic time scale for the breakup of a liquid cylinder driven by the Rayleigh instability is

$$\tau = (\rho R_0/\gamma)^{1/2} \quad (3)$$

where ρ is the density of the fluid, R_0 is the initial radius of the fluid cylinder, and γ is the surface tension.[21] When the phenomenon of the Rayleigh instability is applied to viscoelastic materials such as polymers, the viscosity of the materials resists the breakup of the cylinder. The characteristic time of instability for the fastest growing mode is given by

$$\tau_m = \eta R_0/\gamma \quad (4)$$

where τ_m is the characteristic time, η is the viscosity, R_0 is the original radius, and γ is the surface tension.[37] At higher annealing temperatures, the viscosity of the polymer melt is decreased and shorter annealing time is required for the transformation process.

The sizes of the PMMA nanofibers and nanospheres are compared, as shown in the size distribution histograms (Figure 8). The average diameter of the PMMA nanofibers before annealing is ∼155 nm, and the average diameters of the PMMA nanospheres annealed at 100, 120, and 140 °C are ∼317, 367, and 463 nm, respectively. A summary table for PMMA nanofibers annealed in ethylene glycol at different temperatures is shown in Figure 9a. Considering the theory of the Rayleigh instability and assuming that no satellite droplet is formed between the spheres, the diameters of the spheres can be described as $d = 3.78R_0$ where R_0 is the initial cylinder radius.[27,28] By using the average diameter of the PMMA nanofibers (∼155 nm) as $2R_0$, the calculated nanospheres diameter d is ∼293 nm. Figure 9b shows the plot of the nanosphere size versus the annealing temperature. The error bars represent the standard deviations. The size distributions of the nanospheres are mainly caused by the nonuniform sizes of the original pore sizes of the AAO templates. This issue may be resolved by using AAO templates with pores of narrower distributions. For examples, Masuda and Fukuda have developed a two-step anodization process to fabricate AAO templates with hexagonally packed nanopores of regular pore sizes.[16]

The average sizes of nanospheres annealed at different temperatures are ∼310 to 460 nm. No dependency of the sizes on the annealing temperatures is observed, implying that the polymer nanofibers undergo similar transformation pathways even at different annealing temperatures. The red dashed line in Figure 9b indicates the calculated value of the size of the nanospheres at 293 nm. The average sizes of the nanospheres at different annealing temperatures are larger than the calculated value. The discrepancy of the sizes might be due to the following reasons: (1) There might be residual stress present in the polymer nanofibers made by the precipitation method, which can affect the transformation process; (2) some nanospheres might bump into other nanospheres during the annealing process, for example, the diameter increases by $2^{1/3}$ (∼1.26) times if two nanoparticles are combined into one nanoparticle; and (3) the glass transition temperatures of the polymer chains at the surface of the nanofibers might be different from those of the polymer chains at the center of the nanofibers, resulting in the change of the dominant wavelengths during the transformation process. It has to be noted that nanoparticles with smaller sizes might be formed because of the formation satellite or subsatellites drops during the breakup process.[38]

From the theory and the experimental results, a single nanofiber undulates and transforms into many nanospheres. The number of nanospheres (n) is determined by the length of the original nanofiber (l) and the wavelength of the undulation (λ). When the length of the nanofiber is short and close to the wavelength of the undulation, a single nanofiber may transform into only a single nanosphere. This situation may be achieved

by using shorter nanofibers or nanorods instead of longer nanofibers.

The size of the smallest nanospheres that can be generated in this work is ~80 nm. Using sulfuric acid as electrolyte, AAO templates with pore sizes as small as 5 nm can be fabricated.[39] Therefore, nanospheres with the size ~10 nm might be able to be prepared by applying the annealing method in this work. The radius of gyration of polymer chains, however, has to be considered when the pore size of the anodic aluminum oxide template is close to the radius of gyration of the polymer chains. For example, polystyrene with the weight average molecule weight of 100 kg/mol has a radius of gyration of ~9 nm.[40] Therefore, the polymer chains might be difficult to be drawn into the nanopores of the templates when the pore size is smaller than 20 nm.

From the results of annealing the PMMA nanofibers in ethylene glycol at different temperatures and times, a phase diagram can be constructed (see Figure 10). At lower annealing temperatures and shorter annealing times, the nanofiber morphologies are retained, as indicated by the black closed boxes. At higher annealing temperatures and longer annealing times, the nanofibers undulate and transform to nanospheres, as indicated by the blue closed circles. The transition region is also indicated by the red dashed line in Figure 10. At lower annealing temperatures, longer annealing times are required to transform the nanofibers to nanospheres. The graphical illustrations of the transformation mechanism and corresponding SEM images are shown in Figure 11.

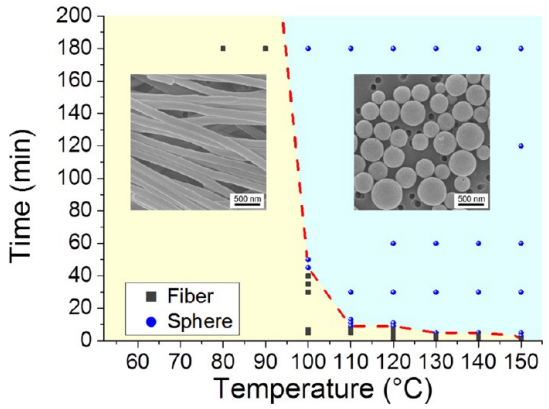

Figure 10. Phase diagram of the PMMA nanostructures by annealing PMMA nanofibers in ethylene glycol at different temperatures for different times. The black closed boxes indicate that fiber morphologies are maintained, while the blue closed circles indicate that spherical morphologies are observed.

The results from this work can be compared to those from our previous work in which microfibers are fabricated by electrospinning.[32] In this work, the measured values of the sphere diameters are larger than the calculated value (~293 nm) of the sphere diameter from the theory, while the measured values agree well with the theoretical values in the experiments using electrospun polymer fibers. The difference may be caused by the preparation methods of the polymer fibers, since the conformations of the polymer chains strongly depend on the preparation conditions that can affect the transformation process of the polymer fibers.

In an attempt to fabricate polymer/titania nanoparticles, we have also tried to encapsulate titania precursors (titanium isopropoxide, TTIP) in polyvinylpyrrolidone (PVP) nanofibers. But the transformation could not be induced by either thermal or solvent annealing. We think that the titania precursor may diffuse to the interface between the polymer fibers and the surrounding medium and inhibit the transformation driven by the Rayleigh instability. One of our future works is to use polymer blends (PS and PMMA) instead of homopolymers. After the staining process by using agents such as RuO_4, the electron density contrast might provide more information about the transformation process driven by the Rayleigh instability.

CONCLUSION

In conclusion, we investigate the annealing effect on PMMA nanofibers made from anodic aluminum oxide (AAO) templates and their transformation to polymer nanospheres. The nanofibers are thermally annealed in ethylene glycol, a nonsolvent for PMMA, and the substrate effect is prevented. During the thermal annealing process, the surfaces of the PMMA nanofibers undulate and transform to nanospheres driven by the Rayleigh instability to minimize the total interfacial energy. A phase diagram is constructed for the nanofibers annealed at different temperatures and times. The characteristic time of the transformation process is shorter because of the lower polymer viscosity.

This work not only studies the annealing effect on one-dimensional polymer nanomaterials, but also provides a simple route for preparing polymer nanospheres. For possible future work, we would like to apply the transformation process of polymer nanofibers to other materials or structures, such as block copolymers, polymer blends, metals, or inorganic materials.

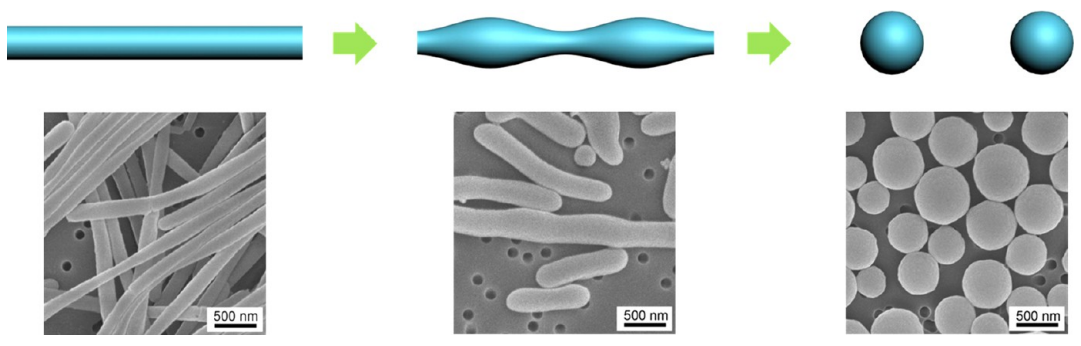

Figure 11. Graphical illustrations and SEM images of polymer nanofibers, undulated polymer structures, and polymer nanospheres.

dx.doi.org/10.1021/am400029j | ACS Appl. Mater. Interfaces 2013, 5, 3134−3142

■ ASSOCIATED CONTENT

Supporting Information

SEM images of AAO templates and PMMA nanostructures annealed at different temperatures. This material is available free of charge via the Internet at http://pubs.acs.org.

■ AUTHOR INFORMATION

Corresponding Author

*E-mail: jtchen@mail.nctu.edu.tw. Tel.: 886-3-5731631.

Notes

The authors declare no competing financial interest.

■ ACKNOWLEDGMENTS

This work was supported by the National Science Council.

■ REFERENCES

(1) Li, C.; Bai, H.; Shi, G. Q. *Chem. Soc. Rev.* **2009**, *38*, 2397−2409.
(2) Jang, J.; Springer, V. Conducting polymer nanomaterials and their applications. In *Emissive Materials: Nanomaterials*; Springer-Verlag: Berlin, 2006; Vol. *199*, pp 189−259.
(3) Sershen, S. R.; Westcott, S. L.; Halas, N. J.; West, J. L. *J. Biomed. Mater. Res.* **2000**, *51*, 293−298.
(4) Chen, J. T.; Hsu, C. S. *Polym. Chem.* **2011**, *2*, 2707−2722.
(5) Huang, Z. M.; Zhang, Y. Z.; Kotaki, M.; Ramakrishna, S. *Compos. Sci. Technol.* **2003**, *63*, 2223−2253.
(6) del Campo, A.; Arzt, E. *Chem. Rev.* **2008**, *108*, 911−945.
(7) Noy, A.; Miller, A. E.; Klare, J. E.; Weeks, B. L.; Woods, B. W.; DeYoreo, J. J. *Nano Lett.* **2002**, *2*, 109−112.
(8) Steinhart, M.; Wehrspohn, R. B.; Gosele, U.; Wendorff, J. H. *Angew. Chem., Int. Ed.* **2004**, *43*, 1334−1344.
(9) Martin, C. R. *Acc. Chem. Res.* **1995**, *28*, 61−68.
(10) Zhang, M. F.; Dobriyal, P.; Chen, J. T.; Russell, T. P.; Olmo, J.; Merry, A. *Nano Lett.* **2006**, *6*, 1075−1079.
(11) Steinhart, M.; Wendorff, J. H.; Greiner, A.; Wehrspohn, R. B.; Nielsch, K.; Schilling, J.; Choi, J.; Gosele, U. *Science* **2002**, *296*, 1997−1997.
(12) Martin, J.; Maiz, J.; Sacristan, J.; Mijangos, C. *Polymer* **2012**, *53*, 1149−1166.
(13) Haberkorn, N.; Lechmann, M. C.; Sohn, B. H.; Char, K.; Gutmann, J. S.; Theato, P. *Macromol. Rapid Commun.* **2009**, *30*, 1146−1166.
(14) Chen, J. T.; Lee, C. W.; Chi, M. H.; Yao, I. C. *Macromol. Rapid Commun.* **2013**, *34*, 348−354.
(15) Steinhart, M.; Senz, S.; Wehrspohn, R. B.; Gosele, U.; Wendorff, J. H. *Macromolecules* **2003**, *36*, 3646−3651.
(16) Masuda, H.; Fukuda, K. *Science* **1995**, *268*, 1466−1468.
(17) Li, A. P.; Muller, F.; Birner, A.; Nielsch, K.; Gosele, U. *J. Appl. Phys.* **1998**, *84*, 6023−6026.
(18) Jessensky, O.; Muller, F.; Gosele, U. *Appl. Phys. Lett.* **1998**, *72*, 1173−1175.
(19) Chen, D.; Zhao, W.; Wei, D. G.; Russell, T. P. *Macromolecules* **2011**, *44*, 8020−8027.
(20) Lee, C. W.; Wei, T. H.; Chang, C. W.; Chen, J. T. *Macromol. Rapid Commun.* **2012**, *33*, 1381−1387.
(21) Eggers, J.; Villermaux, E. *Rep. Prog. Phys.* **2008**, *71*, 036601.
(22) Plateau, J. *Trans. Annu. Rep. Simthsonian Inst.* **1873**, 1863−1866.
(23) Rayleigh, L. *Proc. London Math. Soc.* **1878**, *10*, 4−13.
(24) Tomotika, S. *Rep. Prog. Phys.* **1935**, *153*, 322−337.
(25) Nichols, F. A.; Mullins, W. W. *Trans. Met. Soc. AIME* **1965**, *233*, 1840−1848.
(26) Toimil Molares, M. E.; Balogh, A. G.; Cornelius, T. W.; Neumann, R.; Trautmann, C. *Appl. Phys. Lett.* **2004**, *85*, 5337−5339.
(27) He, Q.; Song, W. X.; Moehwald, H.; Li, J. B. *Langmuir* **2008**, *24*, 5508−5513.
(28) Park, H.; Russell, T. P.; Park, S. *J. Colloid Interface Sci.* **2010**, *348*, 416−423.
(29) Chen, J. T.; Zhang, M. F.; Russell, T. P. *Nano Lett.* **2007**, *7*, 183−187.
(30) Chen, D.; Chen, J. T.; Glogowski, E.; Emrick, T.; Russell, T. P. *Macromol. Rapid Commun.* **2009**, *30*, 377−383.
(31) Mei, S. L.; Feng, X. D.; Jin, Z. X. *Macromolecules* **2011**, *44*, 1615−1620.
(32) Fan, P. W.; Chen, W. L.; Lee, T. H.; Chen, J. T. *Macromol. Rapid Commun.* **2012**, *33*, 343−349.
(33) Fan, P. W.; Chen, W. L.; Lee, T. H.; Chiu, Y. J.; Chen, J. T. *Macromolecules* **2012**, *45*, 5816−5822.
(34) de Gennes, P. G.; Brochard-Wyart, F.; Quere, D. *Capillarity and Wetting Phenomena*; Springer: New York, 2004.
(35) Forrest, J. A.; DalnokiVeress, K.; Stevens, J. R.; Dutcher, J. R. *Phys. Rev. Lett.* **1996**, *77*, 2002−2005.
(36) Forrest, J. A.; DalnokiVeress, K.; Dutcher, J. R. *Phys. Rev. E* **1997**, *56*, 5705−5716.
(37) Edmond, K. V.; Schofield, A. B.; Marquez, M.; Rothstein, J. P.; Dinsmore, A. D. *Langmuir* **2006**, *22*, 9052−9056.
(38) Stone, H. A. *Annu. Rev. Fluid Mech.* **1994**, *26*, 65−102.
(39) Popat, K. C.; Mor, G.; Grimes, C. A.; Desai, T. A. *Langmuir* **2004**, *20*, 8035−8041.
(40) Miyaki, Y.; Einaga, Y.; Fujita, H. *Macromolecules* **1978**, *11*, 1180−1186.